CMS Physics Analysis Summary

Contact: cms-pag-conveners-higgs@cern.ch 2013/03/06

Search for the standard model Higgs boson in the Z boson plus a photon channel in pp collisions at $\sqrt{s} = 7$ and 8 TeV

The CMS Collaboration

Abstract

A search for a Higgs boson decaying into a Z boson and a photon is described. The analysis is performed using a dataset recorded by the CMS experiment at the LHC from proton-proton collisions at a centre-of-mass energy of 7 and 8 TeV, corresponding to an integrated luminosity of 5.0 and 19.6 fb^{-1}, respectively. Limits are set on the cross section of a standard model Higgs boson decaying to opposite-sign electron or muon pairs and a photon. The expected exclusion limits at 95% confidence level are between 6 and 19 times the standard model cross section in the mass range of 120 and 150 GeV, and the observed limits are between about 3 and 31 times the standard model cross section.

1 Introduction

A clear observation of a 125-126 GeV resonance decaying into dibosons and consistent with the Higgs boson was reported by the CMS and ATLAS [1, 2] collaborations. Measurements of the basic properties of this resonance, like the mass and the coupling strength to vectors bosons and fermions, are also available. The next priority is to perform measurements that will provide information of the underlying dynamics of the Higgs sector. The $H \to Z\gamma$ decay channel is important for that purpose because its partial width is induced by loops of heavy charged particles, making it sensitive to physics beyond the standard model (SM), just as the $H \to \gamma\gamma$ decay channel. Despite its small branching fraction, which in the SM varies between 0.111% and 0.246% in the mass range of $120 < m_H < 150$ GeV, the LHC experiments should be sensitive to this channel in the near future. The first search for this decay channel at the LHC was recently reported by the CMS collaboration [3]. In that analysis no excess was found and the observed limits on the Higgs production cross section times the $H \to Z\gamma$ branching fraction fluctuated between about 8 and 48 times the standard model cross section.

This paper describes an update to that search for the Higgs boson in the $H \to Z\gamma$ final state, with the Z boson decaying into an electron or a muon pair. The sensitivity of the search is significantly improved with respect to the one presented in Ref. [3], primarily due to the larger data sample at 8 TeV and an increase in the lepton identification efficiencies. The analysis uses data samples corresponding to an integrated luminosity of 5.0 and 19.6 fb^{-1} of proton-proton collisions at a centre-of-mass energy of 7 and 8 TeV, respectively, recorded by the CMS experiment during 2011 and 2012.

2 The CMS Detector

The central feature of the CMS apparatus is a superconducting solenoid, 13 m in length and 6 m in diameter, which provides an axial magnetic field of 3.8 T. Within the field volume there are several particle detection systems. Charged particle trajectories are measured by silicon pixel and silicon strip trackers, covering $0 \leq \phi \leq 2\pi$ in azimuth and $|\eta| < 2.5$ in pseudorapidity, where η is defined as $-\log[\tan\theta/2]$ and θ is the polar angle of the trajectory of the particle with respect to the counterclockwise proton beam direction. A lead-tungstate crystal electromagnetic calorimeter and a brass/scintillator hadron calorimeter surround the tracking volume and cover the region $|\eta| < 3$. They provide the energy measurements of photons, electrons and hadron jets. A lead/silicon-strip preshower detector is located in front of the endcap for the electromagnetic calorimeter. Muons are identified and measured in gas-ionization detectors embedded in the steel return yoke outside the solenoid. The detector is nearly hermetic, allowing energy balance measurements in the plane transverse to the beam direction. A two-tier trigger system selects the most interesting proton-proton collision events for use in physics analysis. A more detailed description of the CMS detector can be found in Ref. [4].

3 Basic Selection

Events with two opposite-sign, same-flavor leptons (e or μ) consistent with a Z-boson decay and a photon are selected, $e^+e^-\gamma, \mu^+\mu^-\gamma$. All particles must be isolated and have transverse momentum, p_T, greater than 20 (10) GeV for the leading (trailing) lepton and 15 GeV for the photon. The electrons (muons) and the photon must have $|\eta| < 2.5$ ($|\eta| < 2.4$). Photons in the barrel-endcap transition region $1.4442 < |\eta| < 1.566$ of the electromagnetic calorimeter are excluded. The dominant backgrounds to $H \to Z\gamma$ consist of the irreducible background from

the SM $Z\gamma$ production, and the reducible backgrounds from final-state-radiation in Z decays and Z+jets, where a jet or a lepton is misidentified as a photon.

Events are required to pass at least one of the dielectron or dimuon high-p_T triggers. Their efficiencies for events containing two leptons satisfying the analysis selection are measured to be 98% and 91% for the eeγ and $\mu\mu\gamma$ channels, respectively.

Due to the high instantaneous luminosity of the LHC, there are multiple interactions per bunch crossing (pileup). Therefore, events are required to have at least one good primary vertex, with the reconstructed longitudinal position within 24 cm of the geometric center of the detector and the transverse position within 2 cm of the beam interaction region. In the case of multiple vertices, the one with the highest scalar sum of the p_T^2 of its associated tracks is chosen. All leptons, which are used to select events, must come from the same primary vertex. Therefore, electrons (muons) tracks are required to have the transverse and longitudinal impact parameters with respect to the primary vertex to be smaller that 2 (2) mm and 2 (5) mm, respectively.

Photon candidates are reconstructed from clusters of channels in the electromagnetic calorimeter around channels with significant energy deposits, which are merged into superclusters. The clustering algorithms result in almost complete recovery of the energy of photons. In the endcaps, the preshower energy is added where the preshower is present ($|\eta| > 1.65$). The observables used in the photon selection are: isolation variables based on the particle flow (PF) algorithm [5], the ratio of hadronic energy in the hadron calorimeter towers behind the supercluster to the electromagnetic energy in the supercluster, the transverse width of the electromagnetic shower, and an electron veto to avoid misidentifying an electron as a photon. The efficiency of the photon identification is measured from $Z \to ee$ data using tag and probe techniques [6], and found to be between 76% and 88% after including the electron veto inefficiencies measured with $Z \to \mu\mu\gamma$ events, where the photon is produced by final-state radiation.

Electron reconstruction starts from clusters of energy deposited in the electromagnetic calorimeter, which are matched to hits in the silicon strip and the pixel detectors. Electrons are identified using variables which include the ratio between the energy deposited in the hadron and the electromagnetic calorimeters, the shower width in η, and the distance between the calorimeter shower and the particle trajectory in the tracker, measured in both η and ϕ. The selection criteria used are optimized [7] to maintain an efficiency of approximately 60% at low transverse momentum (10 GeV) and 90% at high transverse momentum (50 GeV) for electrons from W or Z decays. For the 2012 data sample, the electron identification efficiency is increased by at least 15% for leptons with $|\eta| > 1.479$ independently of their momentum and by at least 10% for electrons with $p_T < 20$ GeV and $|\eta| < 1.479$ using a multivariate analysis. This new selection also allows the recovery of events in the barrel-endcap transition region of the electromagnetic calorimeter. In addition, the electron energy resolution is improved in the 2012 data sample by optimizing the response function [8] resulting into a 10% (30%) improvement in the mass resolution for $Z \to ee$ events in the barrel (endcap).

Muon candidates are reconstructed with a global fit of trajectories using hits in the tracker and the muon system. The muon candidate must have associated hits in the silicon strip and pixel detectors, have segments in the muon chambers, and have a high-quality global fit to the track trajectory. The efficiency for these muon selection criteria is at least 95% [7]. For the 2012 data sample, the muon identification efficiency is increased by at least 15% from changes in the isolation criteria.

Electrons and muons from Z decays are expected to be isolated from other particles. A cone of size $\Delta R \equiv \sqrt{(\Delta\eta)^2 + (\Delta\phi)^2} = 0.4$ is constructed around the lepton momentum direction.

Table 1: Luminosity and observed data yields used in the analysis. Expected signal yields for a 125 GeV SM Higgs boson.

Sample	Luminosity (fb^{-1})	num. of events $100 < m_{\ell\ell\gamma} < 180$ GeV	num. of events $120 < m_{\ell\ell\gamma} < 150$ GeV	num. of events predicted for $m_H = 125$ GeV
2011 ee	4.98	2268	1041	1.2
2011 $\mu\mu$	5.05	2739	1223	1.4
2012 ee	19.62	12482	5534	6.3
2012 $\mu\mu$	19.62	13392	5993	7.0

The lepton relative isolation is quantified by summing the transverse energy (as measured in the calorimeters) and the transverse momentum (as measured in the silicon tracker) of all PF objects within this cone, excluding the lepton, and then dividing by the lepton transverse momentum. The resulting quantity, corrected for additional underlying event activity due to pileup events [5], is required to be less than 0.4 (0.4) for $Z \to e^+e^-$ ($Z \to \mu^+\mu^-$). This requirement rejects misidentified leptons and background arising from hadronic jets. Similarly, to reduce the background from misidentified jets in the photon reconstruction, photon clusters are required to be isolated from other activities. The photon isolation is defined by requiring the scalar sum of the transverse momenta of charged hadrons, neutral hadrons, and photons, identified by the PF reconstruction in a cone of size $\Delta R = 0.3$ around the candidate photon direction, to be smaller than 1.5 (1.2), 1.0 (1.5), and 0.7 (1.0), respectively, for photons in the barrel(endcap) region. These requirements are applied after correcting for pileup.

The invariant mass of at least one $\ell^+\ell^-$ pair is required to be greater than 50 GeV. This condition rejects any contribution from $H \to \gamma\gamma^*$ where an internal conversion of the photon produced a dilepton pair [9]. If two dilepton pairs are present, the one closest to the Z mass is taken. The invariant mass of the $\ell^+\ell^-\gamma$ system, $m_{\ell\ell\gamma}$, is required to be between 100 and 180 GeV. Other conditions that combine the information from the photon and the leptons are: (1) the ratio of the photon transverse energy to $m_{\ell\ell\gamma}$ must be greater than 15/110, this requirement allows us to reject backgrounds without significant loss in signal sensitivity and without introducing a bias in the $m_{\ell\ell\gamma}$ spectrum; (2) the ΔR separation between each lepton and the photon must be greater than 0.4 in order to reject events with initial-state radiation avoiding photon influence lepton isolation; and (3) final-state radiation events are rejected by requiring a minimum of 185 GeV on the sum of $m_{\ell\ell\gamma}$ and $m_{\ell\ell}$.

The observed yields for the basic event selection described above are listed in Table 1. The total yield for all channels combined is shown in Fig. 1 along with the total expected signal for a 125 GeV SM Higgs boson and the sum of the individual fits to be discussed below.

4 Event classes

The sensitivity of the search can be enhanced by subdividing the selected events into classes according to indicators of the expected mass resolution and the signal-to-background ratio, and then combine the results in each class. For this purpose, four mutually exclusive event classes are defined: in terms of the pseudorapidity of the leptons and the photon and on the shower shape of the photon for one of the topologies.

A significant fraction of the signal events are expected to have both leptons and the photon in the barrel, while only a sixth of the signal events have the photon in the endcap. This is

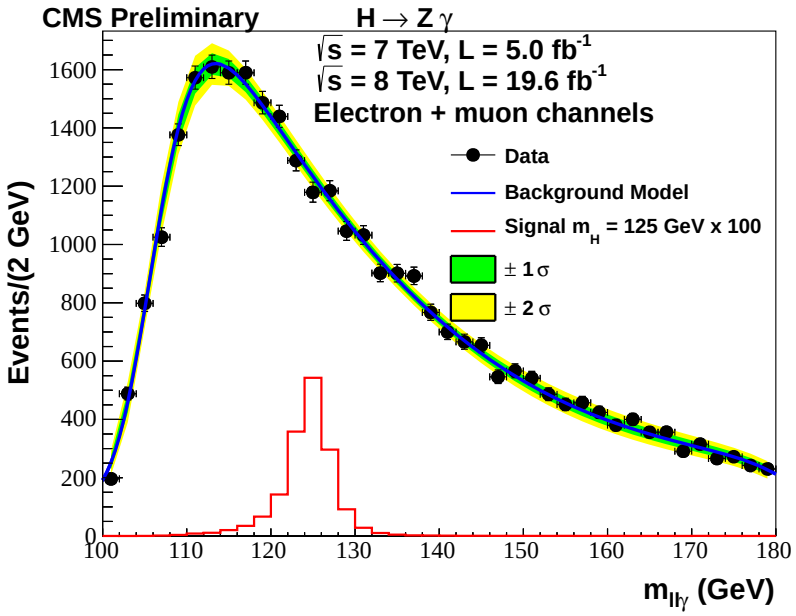

Figure 1: $m_{\ell\ell\gamma}$ spectrum in the electron and the muon channels for the 7 and 8 TeV data combined. Also shown is the expected signal due to a 125 GeV standard model Higgs scaled by 100 and the sum of the individual fits made to the data for each channel and event class.

in contrast with the background, where less than half of the events are in the barrel, while at least a third have a photon in the endcap. In addition events where the photon does not convert have less background and better resolution. For these reasons, the events are classified according to the pseudorapidity of the leptons, the pseudorapidity of the photon and the R_9 value of the photon for events with the two leptons in the barrel. The R_9 variable is defined as the energy sum of 3×3 crystals centered on the most energetic crystal in the supercluster divided by the energy of the supercluster. A high R_9 value, i.e. greater than 0.94, is used to identify unconverted photons.

The exact definition of the four event classes is shown in Table 2, and can be summarized as follows: event classes 1 and 2 have both leptons and the photon in the barrel, but one has the events with high R_9 and the other one low R_9; class 3 events have at least one lepton in the endcap and the photon in the barrel, while class 4 is for all the events with the photon in the endcap. The best signal-to-background is obtained for the event class composed of events with both leptons and the photon in the barrel and high R_9.

5 Background and signal modeling

The background model is obtained by fitting the observed $\ell\ell\gamma$ mass distributions in the electron and the muon channels at 7 and 8 TeV separately for each of the four event classes over the $100 < m_{\ell\ell\gamma} < 180$ GeV range.

Bias studies were performed using pseudo-data generated from background-only fits to the observed $m_{\ell\ell\gamma}$ spectrum. This pseudo-data was fit with combined signal plus a polynomial based background models. Based on that work, a fourth-order polynomial is chosen to fit the event classes where both leptons and the photon are in the barrel, while a fifth-order polynomial is chosen to fit the event classes where at least one lepton is in the endcap and where the photon

Table 2: Definition of the four event classes, the fraction of selected events for a signal with $m_{\mathrm{H}} = 125$ GeV produced by gluon-gluon fusion at 8 TeV and data in a narrow bin centred at 125 GeV. The expected mass resolution on the signal is also shown.

	$e^+e^-\gamma$	$\mu^+\mu^-\gamma$
	Event class 1	
	Photon $0 < \lvert\eta\rvert < 1.4442$ Both leptons $0 < \lvert\eta\rvert < 1.4442$ $R_9 > 0.94$	Photon $0 < \lvert\eta\rvert < 1.4442$ Both leptons $0 < \lvert\eta\rvert < 2.1$ and one lepton $0 < \lvert\eta\rvert < 0.9$ $R_9 > 0.94$
Data	17%	20%
Signal	30%	34%
σ_{eff}	1.9 GeV	1.6 GeV
FWHM	4.5 GeV	3.7 GeV
	Event class 2	
	Photon $0 < \lvert\eta\rvert < 1.4442$ Both leptons $0 < \lvert\eta\rvert < 1.4442$ $R_9 < 0.94$	Photon $0 < \lvert\eta\rvert < 1.4442$ Both leptons $0 < \lvert\eta\rvert < 2.1$ and one lepton $0 < \lvert\eta\rvert < 0.9$ $R_9 < 0.94$
Data	26%	31%
Signal	28%	31%
σ_{eff}	2.1 GeV	1.9 GeV
FWHM	5.0 GeV	4.6 GeV
	Event class 3	
	Photon $0 < \lvert\eta\rvert < 1.4442$ At least one lepton $1.4442 < \lvert\eta\rvert < 2.5$ No requirement on R_9	Photon $0 < \lvert\eta\rvert < 1.4442$ Both leptons in $\lvert\eta\rvert > 0.9$ or one lepton in $2.1 < \lvert\eta\rvert < 2.4$ No requirement on R_9
Data	26%	20%
Signal	23%	18%
σ_{eff}	3.1 GeV	2.1 GeV
FWHM	7.3 GeV	5.0 GeV
	Event class 4	
	Photon $1.566 < \lvert\eta\rvert < 2.5$ Both leptons $0 < \lvert\eta\rvert < 2.5$ No requirement on R_9	Photon $1.566 < \lvert\eta\rvert < 2.5$ Both leptons $0 < \lvert\eta\rvert < 2.4$ No requirement on R_9
Data	31%	29%
Signal	19%	17%
σ_{eff}	3.3 GeV	3.2 GeV
FWHM	7.8 GeV	7.5 GeV

is in the endcap. With these choices and the expected event yield, a possible bias introduced on the limit or the signal strength measurement is negligible. In order to improve the background description below 125 GeV, the $m_{\ell\ell\gamma}$ turn-on distribution for the low mass region is included by fitting a step function multiplied by a polynomial. That product is then convolved with a Gaussian to yield the final shape. The background fits based on the $m_{\ell\ell\gamma}$ data distributions for the electron and muon channels in all event classes are shown in Fig. 2 and Fig. 3, respectively.

The description of the Higgs boson signal used in the search is obtained from simulated events obtained from the next-to-leading order (NLO) matrix-element generator POWHEG [10, 11] interfaced with PYTHIA [12]. The SM Higgs boson cross sections and branching ratios used are taken from Ref. [13].

The simulated signal events are reweighted by taking into account the difference between data

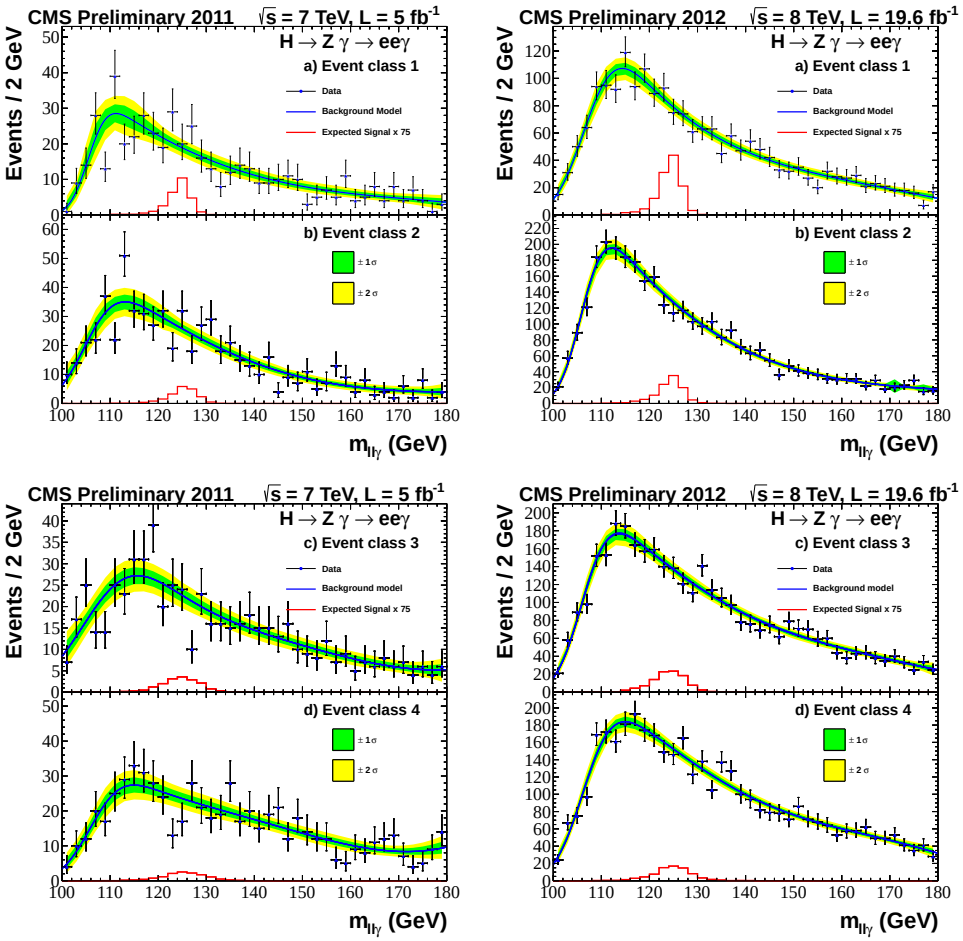

Figure 2: Background model fit to the $m_{ee\gamma}$ distribution for all event classes for the two data samples. The statistical uncertainty bands shown are computed from the data fit.

and simulated events so that the distribution of reconstructed vertices, the trigger efficiencies, the resolution, the energy scale, the reconstruction efficiencies and the isolation efficiency – for the electrons, the muons and the photons – observed in data are reproduced. An additional correction is applied to the photons to reproduce the performance of the R_9 shower shape variable. As an example, the expected signal for a 125 GeV Higgs is shown in Table 1.

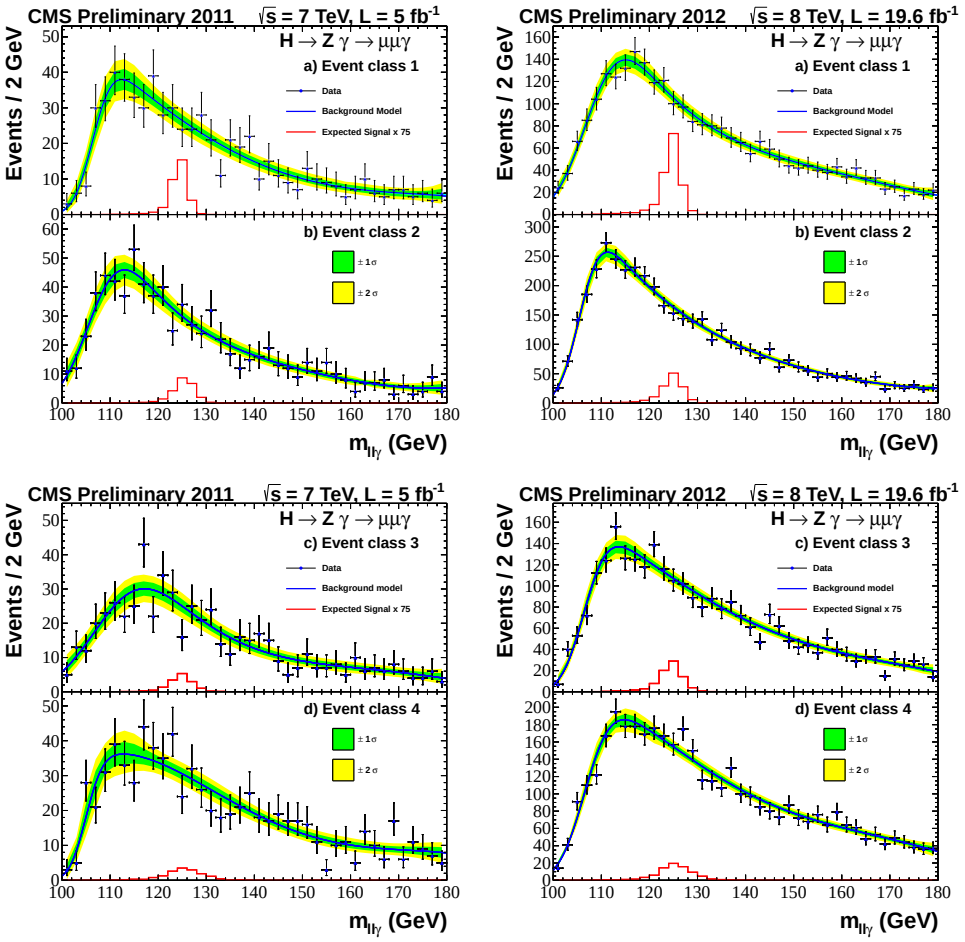

Figure 3: Background model fit to the $m_{\mu\mu\gamma}$ distribution for all event classes for the two data samples. The statistical uncertainty bands shown are computed from the data fit.

6 Results

No evidence of a Higgs boson is observed, and therefore the data are used to derive upper limits on the proton-proton Higgs boson production cross section times the $H \to Z\gamma$ branching fraction, $\sigma(pp \to H)\, Br(H \to Z\gamma)$. The limits are evaluated using a modified frequentist approach, CL_S, taking the profile likelihood as a test statistic [14–16]. An unbinned evaluation of the likelihood is considered.

Table 3 lists the sources of systematic uncertainty considered in the analysis, together with the magnitude of the variation of the source that has been applied. The systematic uncertainties come from the uncertainty on the luminosity measurement [17, 18], the trigger efficiency, choice of parton distribution functions on the signal cross section [19–22], the uncertainty in the Higgs branching fraction prediction [13], the event pileup, the corrections applied to the simulation

Table 3: Separate sources of systematic uncertainties accounted for in the analysis of the 7 and 8 TeV data set. The magnitude of the variation of the source that has been applied to the signal model is shown.

Source	7 TeV	8 TeV
Integrated luminosity	2.2%	4.4%
Theory		
- Gluon-gluon fusion cross section (scale)	+12.5% -8.2%	+7.6% -8.2%
- Gluon-gluon fusion cross section (PDF)	+7.9% -7.7%	+7.6% -7.0%
- Vector boson fusion cross section (scale)	+0.5% -0.3%	+0.3% -0.8%
- Vector boson fusion cross section (PDF)	+2.7% -2.1%	+2.8% -2.6%
- W associate production (scale)	+0.7% -0.8%	+0.2% -0.7%
- W associate production (PDF)	+3.5% -3.5%	+3.5% -3.5%
- Z associate production (scale)	+1.7% -1.6%	+1.9% -1.7%
- Z associate production (PDF)	+3.7% -3.7%	+3.9% -9.7%
- Top pair associate production (scale)	+3.4% -9.4%	+3.9% -9.3%
- Top pair associate production (PDF)	+8.5% -8.5%	+7.9% -7.9%
Branching fraction	6.7%,9.4% -6.7%,-9.3%	6.7%,9.4% -6.7%,-9.3%
Trigger		
- Electron	0.5%	2.0%
- Muon	0.5%	3.5%
Selection		
- Photon Barrel	0.5%	0.6%
- Photon Endcap	1.0%	1.0%
- Electron	0.8%	0.8%
- Muon	0.7%	1.4%
Signal scale and resolution		
- Mean	1.0%	1.0%
- Sigma	5.0%	5.0%
Event migration	5.0%	5.0%
Pileup		
- Electron	0.6%	0.8%
- Muon	0.4%	0.4%

to reproduce the performance of the leptons and photon selections, event migration caused by the requirements on the photon shower shape in the event classification, and signal modeling. The statistical and systematic uncertainties for the corrections are assumed to be uncorrelated. Based on the fit bias studies, the uncertainty on the background estimation due to the chosen functional form is assumed to be negligible.

The expected and observed limits are both shown in Fig. 4. The limits are calculated at 0.5 GeV intervals in the mass range of $120 < m_{\mathrm{H}} < 150$ GeV. The expected exclusion limits at 95% confidence level are between 6 and 19 times the standard model cross section and the observed limit fluctuates between about 3 and 31 times the standard model cross section.

7 Summary

A search has been performed for a SM Higgs boson decaying into a Z-boson and a photon. The analysis has used a dataset from proton-proton collisions at a centre-of-mass energy of 7 and 8 TeV, corresponding to an integrated luminosity of 5.0 and 19.6 fb^{-1}, respectively. No excess has been found and the first limits on the Higgs production cross-section times the $\mathrm{H} \to \mathrm{Z}\gamma$ branching fraction at the LHC have been derived. The expected exclusion limits at 95% confidence level are between 6 and 19 times the standard model cross section in the mass range

of 120 and 150 GeV, and the observed limit fluctuates between about 3 and 31 times the standard model cross section.

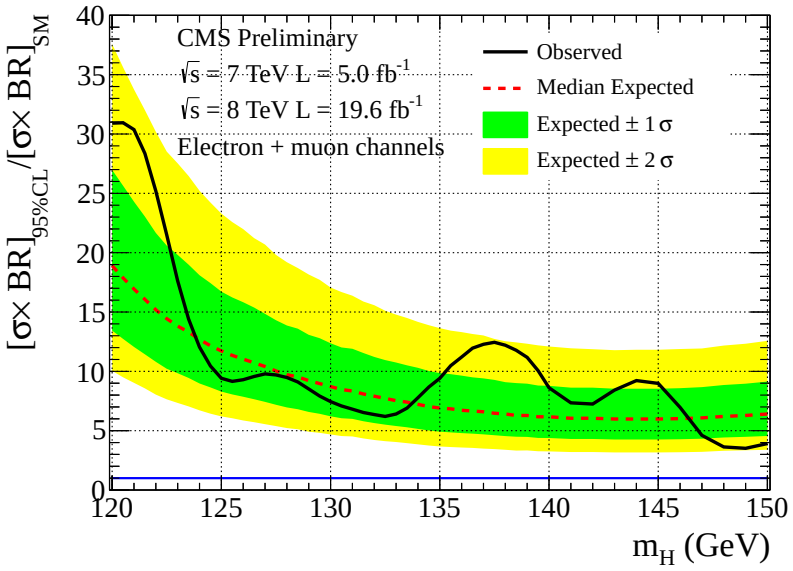

Figure 4: Exclusion limit on the cross section of a SM Higgs boson decaying into Z-boson and a photon as a function of the Higgs boson mass based on 5.0 fb^{-1} of data taken at 7 TeV and 19.6 fb^{-1} at 8 TeV.

References

[1] CMS Collaboration, "Observation of a new boson at a mass of 125 GeV with the CMS experiment at the LHC", *Phys. Lett. B* **716** (2012) 30–61, doi:10.1016/j.physletb.2012.08.021, arXiv:1207.7235.

[2] ATLAS Collaboration, "Observation of a new particle in the search for the Standard Model Higgs boson with the ATLAS detector at the LHC", *Phys. Lett. B* **716** (2012) 1–29, doi:10.1016/j.physletb.2012.08.020, arXiv:1207.7214.

[3] CMS Collaboration, "Search for a Light Higgs boson in the Z boson plus a Photon Decay Channel", *CMS Physics Analysis Summary* **CMS-PAS-HIG-12-049** (2012).

[4] CMS Collaboration, "The CMS experiment at the CERN LHC", *JINST* **3** (2008) S08004, doi:10.1088/1748-0221/3/08/S08004.

[5] CMS Collaboration, "Particle–Flow Event Reconstruction in CMS and Performance for Jets, Taus, and $E_{\mathrm{T}}^{\mathrm{miss}}$", CMS Physics Analysis Summary CMS-PAS-PFT-09-001, (2009).

[6] CMS Collaboration, "Measurement of the inclusive W and Z production cross sections in pp collisions at $\sqrt{s} = 7$ TeV with the CMS experiment", *JHEP* **10** (2011) 132.

[7] CMS Collaboration, "Measurements of inclusive W and Z cross sections in pp collisions at $\sqrt{s} = 7$ TeV", *JHEP* **01** (2011) 080, doi:10.1007/JHEP01(2011)080, arXiv:1012.2466.

[8] CMS Collaboration, "Updated results on the new boson discovered in the search for the standard model Higgs boson in the ZZ to 4 leptons channel in pp collisions at $\sqrt{s} = 7$ and 8 TeV", *CMS Physics Analysis Summary* **CMS-PAS-HIG-12-041** (2012).

[9] A. Firan and R. Stroynowski, "Internal conversions in Higgs decays to two photons", *Phys. Rev. D* **76** (2007) 057301, doi:10.1103/PhysRevD.76.057301, arXiv:0704.3987.

[10] S. Alioli et al., "NLO Higgs boson production via gluon fusion matched with shower in POWHEG", *JHEP* **04** (2009) 002, doi:10.1088/1126-6708/2009/04/002, arXiv:0812.0578.

[11] P. Nason and C. Oleari, "NLO Higgs boson production via vector-boson fusion matched with shower in POWHEG", *JHEP* **02** (2010) 037, doi:10.1007/JHEP02(2010)037, arXiv:0911.5299.

[12] T. Sjöstrand et al., "PYTHIA 6.4 physics and manual", *JHEP* **05** (2006) 026, doi:10.1088/1126-6708/2006/05/026, arXiv:hep-ph/0603175.

[13] LHC Higgs Cross Section Working Group Collaboration, "Handbook of LHC Higgs Cross Sections: 1. Inclusive Observables", arXiv:1101.0593.

[14] A. L. Read, "Presentation of search results: the CL_s technique", *J. Phys. G* **28** (2002) 2693, doi:10.1088/0954-3899/28/10/313.

[15] T. Junk, "Confidence level computation for combining searches with small statistics", *Nucl. Instrum. Meth. A* **434** (1999) 435, doi:10.1016/S0168-9002(99)00498-2, arXiv:hep-ex/9902006.

[16] "Procedure for the LHC Higgs boson search combination in summer 2011", Technical Report ATL-PHYS-PUB-2011-011, CERN, Geneva, (Aug, 2011).

[17] CMS Collaboration, "Absolute Calibration of the Luminosity Measurement at CMS: Winter 2012 Update", CMS Physics Analysis Summary CMS-PAS-SMP-12-008, (2012).

[18] CMS Collaboration, "CMS Luminosity Based on Pixel Cluster Counting - Summer 2012 Update", CMS Physics Analysis Summary CMS-PAS-LUM-12-001, (2012).

[19] M. Botje et al., "The PDF4LHC Working Group Interim Recommendations", arXiv:1101.0538.

[20] S. Alekhin et al., "The PDF4LHC Working Group Interim Report", arXiv:1101.0536.

[21] H.-L. Lai et al., "New parton distributions for collider physics", *Phys. Rev. D* **82** (2010) 074024, doi:10.1103/PhysRevD.82.074024, arXiv:1007.2241.

[22] A. Martin et al., "Parton distributions for the LHC", *Eur. Phys. J. C* **63** (2009) 189–285, doi:10.1140/epjc/s10052-009-1072-5, arXiv:0901.0002.